



Structural analysis of phenyl-germanium, -tin, and -lead dithiocarboxylates $[(RCSS)_xMPh_{4-x}]$, M = Ge, Sn, Pb; $x = 1-3$: affinity between thiocarbonyl sulfur and Group 14 elements

Shinzi Kato ^{a,*}, Kazuyasu Tani ^a, Nobuyuki Kitaoka ^a, Kohzaburoh Yamada ^b,
Hiroyuki Mifune ^b

^a Department of Chemistry, Faculty of Engineering, Gifu University, 1-1 Yanagido, Gifu 501-1193, Japan

^b Fuji Photo Film Co., Ltd., Ashigara Research Laboratories, 210 Nakanuma, Minamiashigara, Kanagawa 250-0193, Japan

Received 25 January 2000; accepted 15 March 2000

Abstract

A series of $RCSSGePh_3$, $(RCSS)_2GePh_2$, $(RCSS)_3SnPh$, and $(RCSS)_2PbPh_2$ were synthesized, and the structures of some *p*-tolyl derivatives $[RCSSMPh_3]$ ($R = 4\text{-CH}_3C_6H_4$, M = Ge; **1d**, Sn: **3d**, Pb: **6d**) and a *o*-tolyl derivative $[(2\text{-CH}_3C_6H_4CSS)_3SnPh]$ (**5c**) were analyzed by X-ray. The results indicate intramolecular non-bonded interactions between the thiocarbonyl sulfur and the central Group 14 element metals. The mono dithiocarboxylates (**1d**, **3d**, and **6d**) exhibit a distorted tetrahedral structure around the central Group 14 elements. Diphenyltin bis(dithiocarboxylate) (**4d**) is shown to take a distorted octahedron or skewed trapezoidal bipyramidal, where the two dithiocarboxylate groups are bound to the Sn atom as an anisobidentate ligand, and the tin tris(dithiocarboxylate) (**5c**) exhibits a seven-coordinated pentagonal bipyramidal. The distance between the thiocarbonyl sulfur and the Sn atom in $4\text{-CH}_3C_6H_4CSSMPh_3$ (M = Ge, Sn, Pb) is shorter than those in the corresponding germanium and lead derivatives. Based on these distances, the affinity of Group 14 elements for sulfur atoms is deduced to decrease in the order Sn > Pb ≥ Ge > Si > C. © 2000 Elsevier Science S.A. All rights reserved.

Keywords: Dithiocarboxylates; X-ray structural analysis; Intramolecular interaction; Affinity

1. Introduction

In contrast to Group 14 element derivatives of dithiocarbamates, dithiocarbonates, and dithiophosphonates, little is known about the corresponding dithiocarboxylate derivatives [1]. Previously, we reported the synthesis of triphenyl-tin [2b] and lead arenecarbodithioates [2d] and diphenyltin bis(arenecarbodithioates) [2b]. The corresponding germanium derivatives ($RCSSGePh_3$, $(RCSS)_2GePh_2$) have not yet been synthesized. In addition, there has been no report of the X-ray structural analysis of organo-Group 14 element derivatives of dithiocarboxylates ($(RCSS)_xMR'_{4-x}$, (R, R' = alkyl, aryl; M = Si, Ge, Sn, Pb; $x = 1-4$), perhaps due to the difficulty of purification and of obtaining

single crystals. We report here the first X-ray structural analyses of a series of phenyl Group 14 element derivatives of dithiocarboxylates together with the synthesis of phenyl-germanium dithiocarboxylates, phenyltin tris(dithiocarboxylates), and diphenylead bis(dithiocarboxylates).

2. Results and discussion

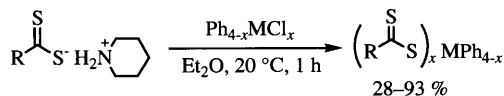
2.1. Synthesis

The stoichiometric reactions of piperidinium dithiocarboxylates with Ph_3GeCl , Ph_2GeCl_2 , $PhSnCl_3$, and Ph_2PbCl_2 proceeded readily at room temperature and led to the quantitative formation of the expected triphenylgermanium dithiocarboxylates **1**, diphenylgermanium bis(dithiocarboxylates) **2**, phenyltin tris(dithiocarboxylates) **5**, and diphenylead bis(dithiocarboxy-

* Corresponding author. Fax: +81-58-2932610.

E-mail address: shinzi@apchem.gifu-u.ac.jp (S. Kato).

lates) **7** (Scheme 1). These dithiocarboxylate derivatives are less crystallizable than the corresponding thiocarboxylate derivatives. After several attempts, we successfully crystallized **1**, **2**, **5**, and **7**, except for triphenylgermanium 2-methylbenzenecarbodithioate (**1c**) and phenyltin tris(dithioacetate) (**5a**). We also attempted the synthesis and isolation of phenylgerma-



No.	M	x	No.	M	x	No.	M	x
1	Ge	1	3	Sn	1	6	Pb	1
2	Ge	2	4	Sn	2	7	Pb	2
			5	Sn	3			
No. R				No. R				
a	CH ₃		d	4-CH ₃ C ₆ H ₄				
b	C ₆ H ₅		e	4-CH ₃ OC ₆ H ₄				
c	2-CH ₃ C ₆ H ₄		f	4-ClC ₆ H ₄				

Scheme 1.

Table 1
Selected bond lengths (Å) and angles (°) of 4-CH₃C₆H₄CSSMPh₃

	Ge (1d)	Sn (3d)	Pb (6d)
<i>Bond lengths</i>			
M1–S11	3.371(l)	3.207(2)	3.362(5)
M1–S12	2.2526(8)	2.446(l)	2.535(4)
C11–S11	1.637(3)	1.645(5)	1.64(2)
C11–S12	1.746(3)	1.737(5)	1.71(l)
M1–C21	1.942(3)	2.137(5)	2.19(2)
M1–C31	1.948(3)	2.146(4)	2.19(l)
M1–C41	1.934(3)	2.124(5)	2.16(2)
<i>Bond angles</i>			
S11–M1–S12	59.71(3)	60.92(4)	57.8(l)
S11–C11–S12	122.2(2)	120.8(3)	122(l)
M1–S11–C11	70.03(10)	76.5(2)	75.6(6)
M1–S12–C11	105.9(l)	100.4(2)	102.6(6)
S12–M1–C21	115.19(9)	119.9(l)	116.2(5)
S12–M1–C31	96.75(8)	94.4(l)	93.9(4)
S12–M1–C41	110.75(9)	109.2(l)	107.8(4)
C21–M1–C31	108.0(1)	114.5(l)	110.1(1)
C21–M1–C41	104.7(2)	117.3(2)	107.9(2)
C31–M1–C41	106.1(6)	119.3(6)	110.5(5)

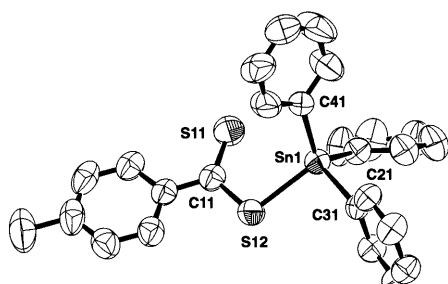


Fig. 1. The ORTEP drawing of 4-CH₃C₆H₄CSSnPh₃ (**3d**). Hydrogen atoms have been omitted for clarity.

nium tris(dithiocarboxylates) ((RCSS)₃GePh) and Group 14 element derivatives of tetrakis(dithiocarboxylates) ((RCSS)₄M, M = Ge, Sn), but failed. For example, the reaction of SnCl₄ with 4 M amounts of sodium or piperidinium 4-methylbenzenecarbodithioate afforded not the desired product **8**, but rather dichlorotin bis(4-methylbenzenecarbodithioate) and bis(4-methylthiobenzoyl) disulfide [3].

2.2. Molecular structures

2.2.1. Mono dithiocarboxylates Group 14 elements derivatives **1**, **3**, and **6**

Selected bond lengths and angles in **1d**, **3d**, and **6d** are collected in Table 1. All molecular forms are similar to the ORTEP drawing of the Sn derivatives **3d** as is shown in Fig. 1. The crystal data are listed in Table 2. The C11–S11 bond lengths (ca. 1.64 Å) are close to the sum of their double bond covalent bond radii [4], and all C11–S12 bond lengths (1.71(1)–1.746(3) Å) are roughly intermediate between their single and double bond covalent bond radii [4]. All M1–S12 bond lengths are also shown in M–S single bonds, respectively [4]. In addition, they are comparable to the distances obtained in germanium-dithiocarbonates [5], tin-dithiocarbonates [6,7], and lead-dithiocarbonates [8] and dithiophosphates [9,10]. The M1–S11 distances are longer than the sum of their covalent bond radii [4], but significantly less than the sum of van der Waals radii of both atoms [11], thus intramolecular interaction should be considered. On the basis of such interaction, the S12–M1–C31 angles significantly deviate from the ideal tetrahedral angle. However, other angles around the central Group 14 elements are relatively comparable to tetrahedral angle. Therefore, mono dithiocarboxylate derivatives show a distorted tetrahedron.

2.2.2. Bis(dithiocarboxylates) Group 14 element derivatives (**4**)

Diphenyltin bis(4-methylbenzenecarbodithioate) (**4d**) crystallized as four independent molecules. The ORTEP drawing and selected bond lengths and angles are shown in Fig. 2 and Table 3. The two dithiocarboxyl groups and the tin atom exist in the same plane. The four C–S bond lengths of the two dithiocarboxylate groups are nearly same values, and are roughly midway between their single and double bond covalent bond radii [4]. The Sn–S bond lengths (av. 2.483(7) Å) are slightly longer than the sum of their covalent bond radii [4], which they are comparable to the distances observed in dimethyltin bis(dithiocarbamates) [12]. On the other hand, the other Sn–S distances (av. 3.056(7) Å) are longer than the sum of their covalent bond radii, which are ca. 0.7 Å shorter than the sum of their van der Waals radii [11] and ca. 0.15 Å shorter than those

Table 2

Crystal data for **1d**, **3d**, **4d**, **5c**, and **6d**

Empirical formula	$C_{26}H_{22}GeS_2$ (1d)	$C_{26}H_{22}S_2Sn$ (3d)	$C_{28}H_{24}S_4Sn$ (4d)	$C_{30}H_{26}S_6Sn$ (5c)	$C_{26}H_{22}PbS_2$ (6d)
Formula weight	471.17	517.27	607.43	697.59	605.78
Crystal system	Triclinic	Triclinic	Monoclinic	Monoclinic	Triclinic
Unit-cell dimensions					
<i>a</i> (Å)	11.224(3)	11.327(2)	9.126(6)	34.703(2)	11.405(3)
<i>b</i> (Å)	12.508(3)	12.306(2)	49.908(8)	10.112(2)	12.434(3)
<i>c</i> (Å)	9.767(3)	9.835(l)	23.955(7)	25.484(2)	9.807(2)
α (°)	90.23(3)	91.21(2)	95.60(5)	137.036(2)	91.44(3)
β (°)	114.70(2)	112.56(1)			112.37(l)
γ (°)	69.33	109.14(1)			110.20(2)
<i>V</i> (Å ³)	1148.7(6)	1178.9(4)	10858(6)	6095.0(9)	1187.2(6)
Space group	$P\bar{1}$ (No. 2)	$P\bar{1}$ (No. 2)	$P2_1/c$ (No. 14)	$C2/c$ (No. 15)	$P\bar{1}$ (No. 2)
<i>Z</i>	2	2	16	8	2
D_{calc} (g cm ⁻³)	1.362	1.457	1.486	1.520	1.694
Crystal size (mm)	0.40 × 0.25 × 0.20	0.10 × 0.10 × 0.45	0.51 × 0.46 × 0.14	0.29 × 0.23 × 0.17	0.23 × 0.14 × 0.09
μ (Mo-K α) (cm ⁻¹)	15.24	12.70	104.74 ^c	12.68	73.03
Temperature (°C)	23.0	23.0	23.0	23.0	23.0
2 <i>θ</i> _{max} (°)	55.0	55.0	119.8	55.0	55.0
Number of measured reflections	4550	5690	17434	7102	5723
Number of unique reflections	4277	5414	16274	6988	5450
<i>R</i> _{int}	0.013	0.024	0.106	0.019	0.080
Number of observations [<i>I</i> >3σ(<i>I</i>)]	3380	3576	5880	4503	1816
Number of variables	262	262	1179	335	262
Reflection/parameter ratio	12.90	13.65	4.99	13.44	6.93
Residuals: <i>R</i> , ^a <i>R</i> _w ^b	0.032, 0.034	0.038, 0.039	0.067, 0.093	0.039, 0.040	0.040, 0.042
<i>P</i> value ^b	0.0150	0.0200	0.0700	0.0150	0.0350
Max. and min. of residual electron density (e Å ⁻³)	0.33, -0.25	0.51, -0.73	0.59, -0.93	0.54, -0.62	0.63, 490
Goodness of fit	1.55	1.42	1.90	1.65	1.07

^a $R = \Sigma(|F_o| - |F_c|)/\Sigma|F_o|$.^b $R_w = [\Sigma w(|F_o| - |F_c|)^2/\Sigma w|F_o|^2]^{1/2}$, $w = [x^2(F_o) + P^2(F_o)^2/4]^{-1}$.^c μ (Cu-K α) (cm⁻¹).

of mono derivative **3d** (3.207(2) Å). The longer Sn–S distances are far apart (S11–Sn–S21 = 152.1(3)°), while the shorter Sn–S distances are close together (S12–Sn–S22 = 84.2(3)°). The S–Sn–C_{ipso} bond angles (106.6(7)–110.4(7)°) are close to the tetrahedral angle, while the C_{ipso}–Sn–C_{ipso} bond angles (129(1)°) are quite different. Since there are two additional Sn–S(x1) interactions, the steric effects of S(x1) would increase the C_{ipso}–Sn–C_{ipso} angles from an ideal tetrahedral angle to 129(1)° and would decrease the S12–Sn–S22 angle to 84.2(3)°. Thus, the two dithiocarboxylate groups are coordinated as anisobidentate ligands toward the tin atom. These results are typical for a highly distorted octahedral or skew trapezoidal bipyramidal structure.

2.2.3. Tris(dithiocarboxylates) Group 14 element derivatives **5**

Although the crystallization of phenyltin tris(4-methylbenzenecarbodithioate) (**5d**) was examined under many different conditions, no suitable single crystals for X-ray structural analysis was obtained. However, we have succeeded in the preparation of single crystals of phenyltin tris(2-methylbenzenecarbodithioate) (**5c**). The

molecular form of **5c** differs from the corresponding thiocarboxylate derivative [13], where the two dithiocarboxyl groups and the tin atom exist in the same plane (Fig. 3(a)). In Table 4, the six C–S bond lengths of the three dithiocarboxyl groups are comparable to those in **4d**, and can be separated into shorter C–S bond lengths (av. 1.661(5) Å) and longer C–S bond lengths (av. 1.701(4) Å). The former are significantly longer than the sum of the double bond covalent bond radii, while the latter are roughly intermediate between

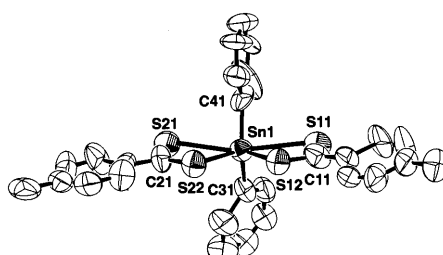


Fig. 2. The ORTEP drawing of one molecule of $(4-\text{CH}_3\text{C}_6\text{H}_4\text{CSS})_2\text{SnPh}_2$ (**4d**). Hydrogen atoms have been omitted for clarity.

Table 3
Selected bond lengths (\AA) and angles ($^\circ$) of diphenyltin bis(4-methylbenzenecarbodithioate) (**4d**)

<i>Bond lengths</i>			
Sn1–S11	3.006(7)	Sn1–S21	3.111(7)
Sn1–S12	2.482(7)	Sn1–S22	2.484(7)
C11–S11	1.69(3)	C21–S21	1.69(3)
C11–S12	1.69(3)	C21–S22	1.66(3)
Sn1–C31	2.07(2)	Sn1–C41	2.07(3)
<i>Bond angles</i>			
Sn11–Sn1–S21	152.1(3)	C31–Sn1–C41	129(l)
Sn12–Sn1–S22	84.2(3)	S21–Sn1–S22	61.8(2)
S11–Sn1–S12	61.9(2)	S21–C21–S22	121(1)
S11–C11–S12	115(1)	Sn1–S21–C21	77.4(7)
Sn1–S11–C11	82.1(9)	Sn1–S22–C21	99(1)
Sn1–S12–C11	100.1(10)	S22–Sn1–C31	107.6(7)
S12–Sn1–C31	110.4(7)	S22–Sn1–C41	108.6(7)
S12–Sn1–C41	106.6(7)		

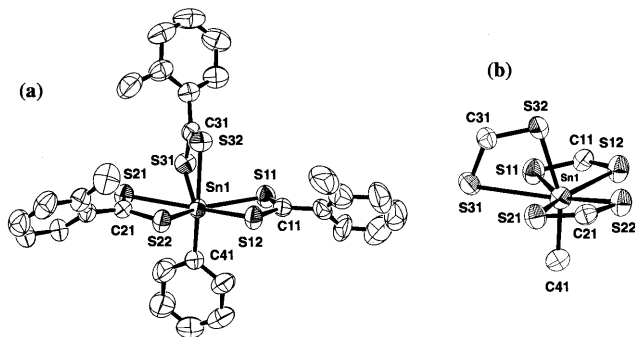


Fig. 3. The ORTEP drawing of $(2\text{-CH}_3\text{C}_6\text{H}_4\text{CSS})_3\text{SnPh}$ (**5c**) (a). The coordination surrounding the Sn1 atom (b). Hydrogen atoms have been omitted for clarity.

Table 4
Selected bond lengths (\AA) and angles ($^\circ$) of phenyltin tris(2-methylbenzenecarbodithioate) (**5c**)

<i>Bond lengths</i>			
Sn1–S11	2.813(1)	Sn1–S12	2.594(1)
Sn1–S21	2.751(1)	Sn1–S22	2.600(1)
Sn1–S31	2.987(1)	Sn1–S32	2.492(1)
Sn1–C41	2.138(1)		
C11–S11	1.663(5)	C12–S11	1.701(4)
C21–S21	1.673(5)	C22–S21	1.691(4)
C31–S31	1.648(4)	C32–S31	1.712(4)
<i>Bond angles</i> ($^\circ$)			
S11–Sn1–S12	65.00(4)	Sn1–S11–C11	84.3(2)
S11–Sn1–S21	144.43(4)	Sn1–S12–C11	90.8(2)
S11–Sn1–S31	72.22(4)	S11–C11–S12	119.9(3)
S12–Sn1–S22	82.79(4)	Sn1–S21–C21	79.4(2)
S12–Sn1–S32	90.87(4)	Sn1–S22–C21	94.6(2)
S12–Sn1–C41	101.5(1)	S21–C21–S22	121.9(3)
S21–Sn1–S22	66.00(4)	S31–Sn1–S32	64.10(4)
S21–Sn1–S31	72.22(4)	S32–Sn1–C41	160.7(1)
S22–Sn1–S32	95.33(5)	Sn1–S31–C31	84.5(2)
S22–Sn1–C41	100.8(1)	Sn1–S32–C31	89.1(2)
		S31–C31–S32	120.3(3)

their single and double bond covalent bond radii [4]. The Sn–S bond lengths of the two dithiocarboxylate groups in the same plane are av. 2.597(1) \AA and av. 2.794(1) \AA , respectively, which are close to the distances observed in divalent tin compounds with bidentate ligands [14,15]. Therefore, these seem to be coordinated in a bidentate form toward the tin atom. The Sn–S bond lengths of the remaining dithiocarboxylate group are 2.492(1) and 2.987(1) \AA , respectively, where the former is close to the smallest Sn–S bond lengths observed in tris(dithiocarbamate) tin derivatives [16]. On the other hand, the latter is the longest of the six Sn–S bond lengths, and is longer than the sum of their covalent bond radii [4]. However, these are shorter than the sum of their van der Waals radii [11], and are also shorter than those of **3d** (3.207(2) \AA) and **4d** (av. 3.056(7) \AA). The S11–Sn1–S21 angle (72.22(4) $^\circ$) is comparable to the ideal pentagonal angle, and the S32–Sn1–C41 angle (160.7(1) $^\circ$) is approximately linear. These results are consistent with a seven-coordinated pentagonal bipyramidal structure, where the S11, S12, S21, S22, and S31 atoms are equatorial and S32 and C41 are axial (Fig. 3(b)).

2.3. Comparison of germanium, tin, and lead dithiocarboxylates

The results from X-ray structural analyses have been explained as follows. In the mono derivatives **1d**, **3d**, and **6d**, the shorter C–S bond lengths are nearly the same (1.637(3)–1.645(5) \AA), while the longer C–S bond lengths slightly shorten in the order Ge > Sn > Pb. Presumably, delocalization of the dithiocarboxylate group may occur in the lead derivative **6d**. The shorter M–S bond lengths indicate single bonds. It is noteworthy that the distance between the sulfur of the shorter C–S bond (thiocarbonyl sulfur) and the central tin atom is shorter than S···Ge and S···Pb distances. The ratio of these distances and the sum of the corresponding van der Waals radii [11] become smaller in the order Sn **3d** (19%) > Pb **6d** (12%) \geq Ge **1d** (11%). This suggests that the electron affinity of the tin atom for the sulfur atom is much stronger than those of the germanium and lead atoms. Sulfur does not generally show a stronger affinity with silicon than oxygen [17]. In $\text{CH}_3\text{C}(\text{S})\text{OSiH}_3$, the distance between the thiocarbonyl sulfur and the silicon atom is 3.185(9) \AA , indicating very weak interaction, although less than the van der Waals distance [11]. Thus, the affinity between sulfur atom and Group 14 elements may decrease in the order Sn > Pb \geq Ge > Si > C. These non-bonding interactions are considered to reflect interaction between the sulfur lone-pair and the non-bonding orbital (σ^* orbital) of C–M or S–M (M = Ge, Sn, Pb). In comparing mono **3d**, bis **4d**, and tris derivatives **5c**, the two C–S bond lengths of **4d** and **5c** are nearly same value, which

suggests that the dithiocarboxylate groups in **4d** and **5c** seem more strongly delocalized than those of **3d**. The Sn–S bond lengths increase in the order **4d** < **3d** < **5c**, but the distances between the thiocarbonyl sulfur and the tin atoms shorten in the order **3d** > **4d** > **5c**. The bidentate characters of dithiocarboxylate groups are considered to increase with their number.

2.4. Spectra

Thiocarbonyl stretching frequencies in the germanium, tin, and lead derivatives are observed at 1160–1200 cm⁻¹ for aliphatic derivatives and 1210–1270 cm⁻¹ for aromatic ones. The ¹³C=S chemical shifts appear at δ 230–250, and those of aliphatic are at lower frequencies than those of aromatic. The ¹¹⁹Sn-NMR chemical shifts are observed at δ –125 to –130 for mono derivatives **3**, δ –250 to –400 for bis derivatives **4**, and δ –650 to –740 for tris derivatives **5**, and those of aliphatic derivatives are at a lower field than those of aromatic derivatives. The coupling constants of tin–carbon appear at 600 Hz and 800 Hz, respectively, with a difference of 200 Hz. The thiocarbonyl stretching frequencies and the thiocarbonyl carbon and ¹¹⁹Sn chemical shifts of 4-methylbenzene derivatives are shown in Table 5. The thiocarbonyl stretching frequencies are nearly the same, but the ¹³C=S chemical shifts show 3 ppm downfield shift with an increase in dithiocarboxylate groups. On the other hand, the ¹¹⁹Sn chemical shifts show upfield shifts in the order **3d** < **4d** < **5d**, with a difference of 250 ppm between **3d** and **4d** and of 350 ppm between **4d** and **5d**. In these spectroscopic data of mono-, bis-, and tris(4-methylbenzenecarboxylates) germanium, tin, and lead derivatives, the ν(C=S) stretching frequencies are nearly the same, but the ¹³C=S chemical shifts are in the order Ge < Sn < Pb and mono- < bis- < tris(dithiocarboxylate) derivatives.

Table 5
Selected features in the spectroscopic data of (4-CH₃C₆H₄CSS)_x-MPh_{4-x}^a

No.	M	x	ν(C=S) ^b (cm ⁻¹)	δ _{C-S} ^c	δ ₁₁₉ Sn ^d
1d	Ge	1	1220, 1212	227.7	
3d	Sn	1	1242, 1224	232.1	–138.8
6d	Pb	1	1219, 1210	234.5	
2d	Ge	2	1238, 1221	228.0	
4d	Sn	2	1239, 1221	235.9	–392.0
7d	Pb	2	1222	239.4	
5d	Sn	3	1242, 1224	238.2	–739.5

^a Standard: Me₄Sn.

^b In KBr.

^c In CDCl₃.

^d In C₆D₆.

3. Conclusion

A series of germanium, tin, and lead derivatives of dithiocarboxylates were synthesized, and their structures were analyzed by X-ray. These molecules show the existence of intramolecular non-bonding interactions between the thiocarbonyl sulfur atoms and the central Group 14 element metals. Comparative studies of the compounds RCSSMPh₃ (M = Ge, Sn, Pb) revealed that the distance between the thiocarbonyl sulfur and the tin atom is shorter than those of the germanium and lead derivatives. These non-bonding interactions reflect the affinity between the sulfur atoms and the Group 14 elements, i.e. this affinity decreases in the order Sn > Pb ≥ Ge > Si > C. Such order of the affinity would contribute not only to the synthesis of the relevant compounds but also elucidation of biological mechanism in which the Group 14 elements and sulfur participate.

4. Experimental

Melting points were determined by a Yanagimoto micromelting point apparatus, but not corrected. The IR spectra were measured on Perkin–Elmer FT-IR 1640 spectrophotometer. ¹H- (400 MHz) and ¹³C-NMR spectra (100 MHz) were measured on a JEOL JNM- α 400 in CDCl₃ containing Me₄Si as an internal standard. ¹¹⁹Sn-NMR spectra (149 MHz) were also measured on a JEOL JNM- α 400 with Me₄Sn as an external standard. UV-vis spectra were obtained from a JASCO U-Best 55. Elemental analyses were performed by the Elemental Analysis Center of Kyoto University. All solvents were dried and distilled prior to use. Ph₃GeCl, Ph₂GeCl₂, Ph₃SnCl, Ph₂SnCl₂, PhSnCl₃, SnCl₄–CH₂Cl₂ 1.0 M solution, and Ph₃PbCl are of commercial grade were obtained from Aldrich. Ph₂PbCl₂ was obtained from Alfa Chemical Co. Piperidinium [18] and sodium dithiocarboxylates [2f] were prepared by previously described methods. A series of RCSSMPh₃ (M = Sn: **3** [2b,f], Pb: **6** [2d]) and (RCSS)₂SnPh₂ **4** [2b] were synthesized according to the procedures reported previously.

4.1. General procedures

The synthesis of triphenylgermanium 4-methylbenzenecarbodithioate (**1d**) is described in detail as a typical procedure for compounds **1**, **2**, **5**, and **7**. For **3** [2b], **4** [2b], and **6** [2d], the additional spectral data and elemental analysis are described.

1a. Recrystallizing solvents: hexane; orange crystals (28%); m.p. 89–90°C. IR (KBr): 1193 (C=S), 1158 (C=S) cm⁻¹. ¹H-NMR (CDCl₃): δ 2.91 (s, 3H, CH₃), 7.39–7.44 (m, 9H, Ar), 7.62–7.65 (m, 6H, Ar). ¹³C-

NMR (CDCl_3): δ 43.8 (CH_3), 128.0, 129.3, 134.7, 136.8, 236.6 (C=S). **UV-vis** (CH_2Cl_2) λ_{\max} ($\log \varepsilon$): 222 (4.05), 289 (3.95), 309 (3.48), 518 (2.13) nm.

1b. Recrystallizing solvents: 1:1 Et_2O –hexane; purple crystals (60%); m.p. 108–110°C. **IR** (KBr): 1218 (C=S) cm^{-1} . **$^1\text{H-NMR}$** (CDCl_3): δ 7.39–7.44 (m, 11H, Ar), 7.68–7.71 (m, 7H, Ar), 8.19–8.22 (m, 2H, Ar). **$^{13}\text{C-NMR}$** (CDCl_3): δ 127.1, 128.0, 128.5, 129.9, 132.5, 134.7, 134.8, 145.7, 228.7 (C=S). **UV-vis** (CH_2Cl_2) λ_{\max} ($\log \varepsilon$): 222 (4.36), 270 (4.46), 306 (4.13), 519 (2.58) nm. Anal. Found: C, 65.62; H, 4.47. $\text{C}_{25}\text{H}_{19}\text{ClGeS}_2$ Calc.: C, 65.68; H, 4.41%.

1c. Reddish–purple oil (88%). **IR** (neat): 1240 (C=S) cm^{-1} . **$^1\text{H-NMR}$** (CDCl_3): δ 2.38 (s, 3H, CH_3), 7.12–7.20 (m, 3H, Ar), 7.32–7.43 (m, 10H, Ar), 7.69–7.71 (m, 6H, Ar). **$^{13}\text{C-NMR}$** (CDCl_3): δ 19.7 (CH_3), 125.5, 125.9, 128.6, 128.8, 130.0, 130.7, 132.2, 134.1, 134.8, 150.1, 235.7 (C=S).

1d. To a solution of Ph_3GeCl (0.339 g, 1.00 mmol) in Et_2O (15 ml), piperidinium 4-methylbenzenecarbodithioate (0.254 g, 1.00 mmol) was added and the mixture was stirred at 20°C for 1 h. After addition of CH_2Cl_2 (100 ml), the mixture was washed with water (3 × 90 ml), followed by drying over MgSO_4 . The solvents were removed under reduced pressure (30°C/2.7 kPa), and the resulting residue was dissolved into a mixed solvent of CH_2Cl_2 (4.0 ml) and hexane (3.0 ml) and allowed to stand in a refrigerator (–20°C) for 24 h to give **1d** as purple crystals (0.306 g, 65%); m.p. 129–130°C. **IR** (KBr): 1220 (C=S), 1212 (C=S) cm^{-1} . **$^1\text{H-NMR}$** (CDCl_3): δ 2.37 (s, 3H, CH_3), 7.15 (d, J = 8.4 Hz, 2H, Ar), 7.39–7.47 (m, 9H, PhGe), 7.73–7.75 (m, 6H, PhGe), 8.19 (d, J = 8.4 Hz, 2H, Ar). **$^{13}\text{C-NMR}$** (CDCl_3): δ 21.5 (CH_3), 127.2, 128.5, 128.7, 129.8, 134.6, 134.8, 143.2, 143.5, 227.7 (C=S). **UV-vis** (CH_2Cl_2) λ_{\max} ($\log \varepsilon$): 222 (4.46), 273 (4.71), 320 (4.27), 527 (2.65) nm. Anal. Found: C, 66.30; H, 4.75. $\text{C}_{26}\text{H}_{22}\text{GeS}_2$ Calc.: C, 66.27; H, 4.71%.

1e. Recrystallizing solvents: 1:1 CH_2Cl_2 –hexane; purple crystals (60%); m.p. 117–118°C. **IR** (KBr): 1261 (C=S), 1243 (C=S), 1228 (C=S) cm^{-1} . **$^1\text{H-NMR}$** (CDCl_3): δ 3.79 (s, 3H, CH_3O), 6.78 (d, J = 8.9 Hz, 2H, Ar), 7.36–7.43 (m, 9H, PhGe), 7.69–7.71 (m, 6H, PhGe), 8.28 (d, J = 8.9 Hz, 2H, Ar). **$^{13}\text{C-NMR}$** (CDCl_3): δ 55.5 (CH_3O), 113.0, 128.0, 128.4, 129.5, 129.8, 134.8, 138.9, 163.8, 225.5 (C=S). **UV-vis** (CH_2Cl_2) λ_{\max} ($\log \varepsilon$): 222 (4.50), 270 (5.42), 341 (4.40), 520 (2.81) nm. Anal. Found: C, 64.36; H, 4.75. $\text{C}_{26}\text{H}_{22}\text{GeOS}_2$ Calc.: C, 64.10; H, 4.55%.

1f. Recrystallizing solvents: 4:3 CH_2Cl_2 –hexane; purple crystals (57%); m.p. 120–121°C. **IR** (KBr): 1211 (C=S) cm^{-1} . **$^1\text{H-NMR}$** (CDCl_3): δ 7.23 (d, J = 8.3 Hz, 2H, Ar), 7.31–7.36 (m, 9H, PhGe), 7.60–7.62 (m, 6H, PhGe), 8.08 (d, J = 8.3 Hz, 2H, Ar). **$^{13}\text{C-NMR}$** (CDCl_3): δ 128.0, 128.1, 128.4, 128.6, 130.0, 134.2, 134.4, 134.9, 226.6 (C=S). **UV-vis** (CH_2Cl_2) λ_{\max}

($\log \varepsilon$): 222 (4.35), 273 (4.13), 316 (4.24), 531 (2.59) nm. Anal. Found: C, 61.17; H, 3.95. $\text{C}_{25}\text{H}_{19}\text{ClGeS}_2$ Calc.: C, 61.08; H, 3.90%.

2a. Recrystallizing solvents: hexane; orange crystals (54%); m.p. 78–79°C. **IR** (KBr): 1197 (C=S), 1183 (C=S) cm^{-1} . **$^1\text{H-NMR}$** (CDCl_3): δ 2.61 (s, 6H, CH_3), 7.15 (t, J = 6.6 Hz, 4H, PhGe), 7.38 (t, J = 6.6 Hz, 4H, PhGe), 7.48 (d, J = 6.6 Hz, 2H, PhGe). **$^{13}\text{C-NMR}$** (CDCl_3): δ 45.7 (CH_3), 128.1, 130.2, 133.5, 135.9, 229.4 (C=S). **UV-vis** (CH_2Cl_2) λ_{\max} ($\log \varepsilon$): 222 (4.14), 270 (3.42), 309 (3.39), 409 (3.00), 520 (3.58) nm.

2b. Recrystallizing solvents: 4:3 CH_2Cl_2 –hexane; red crystals (62%); m.p. 196–198°C. **IR** (KBr): 1237 (C=S), 1222 (C=S) cm^{-1} . **$^1\text{H-NMR}$** (CDCl_3): δ 7.31–7.53 (m, 8H, Ar), 7.67–7.74 (m, 2H, PhGe), 7.90–7.96 (m, 6H, Ar), 8.07–8.22 (m, 4H, Ar). **$^{13}\text{C-NMR}$** (CDCl_3): δ 128.3, 128.5, 128.6, 128.7, 128.8, 131.0, 133.2, 133.7, 228.7 (C=S). **UV-vis** (CH_2Cl_2) λ_{\max} ($\log \varepsilon$): 222 (4.39), 270 (4.52), 305 (3.17), 515 (2.63) nm. Anal. Found: C, 58.62; H, 3.81. $\text{C}_{26}\text{H}_{20}\text{GeS}_4$ Calc.: C, 58.55; H, 3.78%.

2c. Red oil (82%). **IR** (neat): 1241 (C=S) cm^{-1} . **$^1\text{H-NMR}$** (CDCl_3): δ 2.31 (s, 6H, CH_3), 7.09–7.96 (m, 18H, Ar). **$^{13}\text{C-NMR}$** (CDCl_3): δ 19.8 (CH_3), 125.5, 126.0, 128.6, 128.8, 129.2, 130.8, 132.5, 133.6, 134.3, 148.8, 235.7 (C=S).

2d. Recrystallizing solvents: 7:5 CH_2Cl_2 –hexane; red crystals (69%); m.p. 114–116°C. **IR** (KBr): 1238 (C=S), 1221 (C=S) cm^{-1} . **$^1\text{H-NMR}$** (CDCl_3): δ 2.34 (s, 6H, CH_3), 7.17 (d, J = 8.1 Hz, 4H, Ar), 7.21 (t, J = 6.9 Hz, 6H, PhGe), 7.31 (d, J = 8.1 Hz, 4H, Ar), 7.48 (d, J = 6.9 Hz, 4H, PhGe). **$^{13}\text{C-NMR}$** (CDCl_3): δ 21.6 (CH_3), 127.1, 128.5, 128.7, 129.1, 130.2, 134.2, 142.2, 144.1, 228.0 (C=S). **UV-vis** (CH_2Cl_2) λ_{\max} ($\log \varepsilon$): 222 (4.41), 271 (4.22), 324 (4.73), 515 (2.52) nm. Anal. Found: C, 60.01; H, 4.33. $\text{C}_{28}\text{H}_{24}\text{GeS}_4$ Calc.: C, 59.91; H, 4.31%.

2e. Recrystallizing solvents: 5:4 CH_2Cl_2 –hexane; red crystals (60%); m.p. 119–121°C. **IR** (KBr): 1240 (C=S) cm^{-1} . **$^1\text{H-NMR}$** (CDCl_3): δ 3.77 (s, 6H, CH_3O), 6.76 (d, J = 9.0 Hz, 4H, Ar), 7.23–7.58 (m, 6H, Ar), 7.81–7.99 (m, 4H, PhGe), 8.02 (d, J = 9.0 Hz, 4H, Ar). **$^{13}\text{C-NMR}$** (CDCl_3): δ 55.5 (CH_3O), 113.5, 128.4, 128.6, 129.3, 133.1, 134.1, 137.8, 164.1, 225.7 (C=S). **UV-vis** (CH_2Cl_2) λ_{\max} ($\log \varepsilon$): 222 (4.42), 272 (4.31), 349 (4.55), 516 (2.83) nm. Anal. Found: C, 56.69; H, 4.10. $\text{C}_{28}\text{H}_{24}\text{GeO}_2\text{S}_4$ Calc.: C, 56.68; H, 4.08%.

2f. Recrystallizing solvents: 4:3 CH_2Cl_2 –hexane; red crystals (62%); m.p. 146–148°C. **IR** (KBr): 1236 (C=S) cm^{-1} . **$^1\text{H-NMR}$** (CDCl_3): δ 7.20 (d, J = 8.7 Hz, 4H, Ar), 7.30–7.50 (m, 6H, PhGe), 7.76–7.81 (m, 4H, PhGe), 8.02 (d, J = 8.7 Hz, 4H, Ar). **$^{13}\text{C-NMR}$** (CDCl_3): δ 128.1, 128.5, 128.6, 130.2, 133.1, 134.1, 139.6, 142.5, 226.4 (C=S). **UV-vis** (CH_2Cl_2) λ_{\max} ($\log \varepsilon$): 222 (4.45), 273 (4.24), 312 (4.28), 516 (2.69) nm. Anal. Found: C, 51.89; H, 3.11. $\text{C}_{26}\text{H}_{18}\text{Cl}_2\text{GeS}_4$ Calc.: C, 51.86; H, 3.01%.

3a. Orange oil (92%). IR (neat): 1187 (C=S), 1174 (C=S), 1152 (C=S) cm⁻¹. ¹H-NMR (CDCl₃): δ 2.94 (s, 3H, CH₃), 7.36–7.40 (m, 9H, PhSn), 7.64–7.67 (m, 6H, PhSn). ¹³C-NMR (CDCl₃): δ 42.0 (CH₃), 128.8, 129.7, 136.5, 136.8, 242.0 (C=S). ¹¹⁹Sn-NMR (CDCl₃): δ –127.4 ($^1J_{C-Sn}$ = 595 Hz). UV-vis (CH₂Cl₂) λ_{max} (log ϵ): 319 (3.94), 461 (1.74) nm.

3b [2b]. Recrystallizing solvents: 5:3 CH₂Cl₂–hexane; red crystals (78%). ¹³C-NMR (CDCl₃): δ 127.9, 128.5, 128.9, 129.7, 136.5, 136.7, 136.8, 143.9, 233.1 (C=S). ¹¹⁹Sn-NMR (CDCl₃): δ –135.4 ($^1J_{C-Sn}$ = 597 Hz). Anal. Found: C, 59.72; H, 4.15. C₂₅H₂₀S₂Sn Calc.: C, 59.66; H, 4.01%.

3c [2b]. Recrystallizing solvents: 1:1 CH₂Cl₂–hexane; red crystals (74%). ¹³C-NMR (CDCl₃): δ 20.1 (CH₃), 125.5, 126.1, 128.9, 129.1, 129.8, 130.8, 132.4, 136.8, 138.7, 148.8, 240.1 (C=S). ¹¹⁹Sn-NMR (CDCl₃): δ –126.5 ($^1J_{C-Sn}$ = 591 Hz). Anal. Found: C, 60.52; H, 4.39. C₂₆H₂₂S₂Sn Calc.: C, 60.37; H, 4.29%.

3d [2b,f]. Recrystallizing solvents: 7:5 CH₂Cl₂–hexane; red crystals (70%).

3e [2b]. Recrystallizing solvents: 5:4 CH₂Cl₂–hexane; red crystals (75%). ¹³C-NMR (CDCl₃): δ 55.5 (CH₃O), 113.0, 128.8, 129.5, 130.1, 134.6, 136.8, 139.8, 164.0, 229.8 (C=S). ¹¹⁹Sn-NMR (CDCl₃): δ –143.1 ($^1J_{C-Sn}$ = 597 Hz). Anal. Found: C, 58.61; H, 4.22. C₂₆H₂₂OS₂Sn Calc.: C, 58.56; H, 4.16%.

3f [2b]. Recrystallizing solvents: 6:5 CH₂Cl₂–hexane; red crystals (69%). ¹³C-NMR (CDCl₃): δ 128.0, 128.7, 129.3, 130.3, 134.7, 141.3, 141.4, 143.6, 230.2 (C=S). ¹¹⁹Sn-NMR (CDCl₃): δ –130.4 ($^1J_{C-Sn}$ = 612 Hz). Anal. Found: C, 55.92; H, 3.66. C₂₅H₁₉ClS₂Sn Calc.: C, 55.84; H, 3.56%.

4a. Recrystallizing solvents: hexane; orange crystals (87%); m.p. 98–99°C. IR (KBr): 1172 (C=S), 1151 (C=S) cm⁻¹. ¹H-NMR (CDCl₃): δ 2.64 (s, 6H, CH₃), 7.24–7.35 (m, 6H, PhSn), 7.48–7.50 (m, 4H, PhSn). ¹³C-NMR (CDCl₃): δ 51.1 (CH₃), 128.7, 129.8, 135.4, 140.5, 252.4 (C=S). ¹¹⁹Sn-NMR (CDCl₃): δ –251.5 ($^1J_{C-Sn}$ = 741 Hz). UV-vis (CH₂Cl₂) λ_{max} (log ϵ): 320 (3.88), 417 (2.11) nm.

4b [2b]. Recrystallizing solvents: 8:5 CH₂Cl₂–hexane; orange crystals (82%). ¹³C-NMR (CDCl₃): δ 127.3, 128.0, 129.0, 130.0, 133.8, 134.7, 142.7, 144.8, 236.9 (C=S). ¹¹⁹Sn-NMR (CDCl₃): δ –385.0 ($^1J_{C-Sn}$ = 817 Hz). Anal. Found: C, 53.96; H, 3.52. C₂₆H₂₀S₄Sn Calc.: C, 53.90; H, 3.48%.

4c. Recrystallizing solvents: 1:1 CH₂Cl₂–hexane; red crystals (70%); m.p. 79–80°C. IR (KBr): 1233 (C=S) cm⁻¹. ¹H-NMR (CDCl₃): δ 2.43 (s, 6H, CH₃), 7.11–7.24 (m, 6H, Ar), 7.41–7.49 (m, 8H, Ar), 7.95–8.01 (m, 4H, Ar). ¹³C-NMR (CDCl₃): δ 20.5 (CH₃), 125.6, 126.7, 129.1, 129.8, 131.0, 133.1, 134.7, 135.8, 144.2, 146.9, 244.2 (C=S). ¹¹⁹Sn-NMR (CDCl₃): δ –367.4 ($^1J_{C-Sn}$ = 805 Hz). UV-vis (CH₂Cl₂) λ_{max} (log ϵ): 338 (4.32), 457 (2.93) nm. Anal. Found: C, 55.39; H, 4.00. C₂₈H₂₄S₄Sn Calc.: C, 55.36; H, 3.98%.

4d [2b]. Recrystallizing solvents: 7:5 CH₂Cl₂–hexane; orange crystals (88%). ¹³C-NMR (CDCl₃): δ 21.7 (CH₃), 127.4, 128.6, 128.8, 129.4, 134.6, 140.3, 145.1, 145.4, 235.9 (C=S). ¹¹⁹Sn-NMR (CDCl₃): δ –392.0 ($^1J_{C-Sn}$ = 807 Hz). Anal. Found: C, 55.44; H, 4.07. C₂₈H₂₄S₄Sn Calc.: C, 55.36; H, 3.98%.

4e. Recrystallizing solvents: 3:2 CH₂Cl₂–hexane; orange crystals (81%); m.p. 169–170°C. ¹H-NMR (CDCl₃): δ 3.81 (s, 6H, CH₃O), 6.78 (d, J = 8.9 Hz, 4H, Ar), 7.32–7.40 (m, 6H, PhSn), 7.90–7.93 (m, 4H, PhSn), 8.32 (d, J = 8.9 Hz, 4H, Ar). ¹³C-NMR (CDCl₃): δ 55.6 (CH₃O), 113.0, 128.8, 129.3, 130.0, 134.6, 136.0, 146.2, 164.9, 233.5 (C=S). ¹¹⁹Sn-NMR (CDCl₃): δ –402.7 ($^1J_{C-Sn}$ = 812 Hz). Anal. Found: C, 52.61; H, 3.82. C₂₈H₂₄O₂S₄Sn Calc.: C, 52.59; H, 3.78%.

4f [2b]. Recrystallizing solvents: 6:5 CH₂Cl₂–hexane; orange crystals (79%). ¹³C-NMR (CDCl₃): δ 128.1, 128.6, 129.1, 129.8, 134.7, 140.6, 141.0, 144.0, 234.6 (C=S). ¹¹⁹Sn-NMR (CDCl₃): δ –378.9 ($^1J_{C-Sn}$ = 826 Hz). Anal. Found: C, 48.22; H, 2.83. C₂₆H₁₈Cl₂S₄Sn Calc.: C, 48.17; H, 2.80%.

5a. Orange oil (41%). IR (neat): 1196 (C=S), 1148 (C=S) cm⁻¹. ¹H-NMR (CDCl₃): δ 2.78 (s, 9H, CH₃), 7.37–7.48 (m, 3H, PhSn), 7.77–7.79 (m, 2H, PhSn). ¹³C-NMR (CDCl₃): δ 48.5 (CH₃), 128.8, 131.6, 134.5, 139.0, 250.5 (C=S). ¹¹⁹Sn-NMR (CDCl₃): δ –652.2. UV-vis (CH₂Cl₂) λ_{max} (log ϵ): 222 (5.12), 270 (4.52), 310 (3.85), 401 (2.75) nm.

5b. Recrystallizing solvents: 5:1:7 CH₂Cl₂–AcOEt–hexane; orange crystals (82%); m.p. 144–147°C. IR (KBr): 1236 (C=S), 1221 (C=S) cm⁻¹. ¹H-NMR (CDCl₃): δ 7.32–7.40 (m, 9H, Ar), 7.54–7.58 (m, 3H, Ar), 8.06–8.08 (m, 2H, Ar), 8.29–8.31 (m, 6H, Ar). ¹³C-NMR (CDCl₃): δ 127.3, 128.1, 129.1, 130.0, 131.1, 134.1, 144.4, 151.8, 239.4 (C=S). ¹¹⁹Sn-NMR (CDCl₃): δ –737.2. UV-vis (CH₂Cl₂) λ_{max} (log ϵ): 222 (4.52), 262 (4.33), 313 (4.96), 445 (3.70) nm. Anal. Found: C, 49.52; H, 3.14. C₂₇H₂₀S₆Sn Calc.: C, 49.47; H, 3.08%.

5c. Recrystallizing solvents: 7:3:8 AcOEt–Et₂O–hexane; orange crystals (85%); m.p. 110–113°C. IR (KBr): 1226 (C=S) cm⁻¹. ¹H-NMR (CDCl₃): δ 2.54 (s, 9H, CH₃), 7.13–7.16 (m, 6H, Ar), 7.23–7.26 (m, 3H, Ar), 7.44–7.46 (m, 3H, Ar), 7.56–7.58 (m, 3H, Ar), 8.08–8.10 (m, 2H, Ar). ¹³C-NMR (CDCl₃): δ 20.9 (CH₃), 125.6, 127.1, 129.1, 130.1, 130.2, 131.1, 131.2, 133.5, 145.0, 151.1, 246.5 (C=S). ¹¹⁹Sn-NMR (CDCl₃): δ –710.7. Anal. Found: C, 51.66; H, 3.73. C₃₀H₂₆S₆Sn Calc.: C, 51.65; H, 3.76%.

5d. Recrystallizing solvents: 2:6:5 CH₂Cl₂–AcOEt–hexane; orange crystals (77%); m.p. 130–132°C. IR (KBr): 1242 (C=S), 1224 (C=S) cm⁻¹. ¹H-NMR (CDCl₃): δ 2.24 (s, 9H, CH₃), 7.04 (d, J = 8.4 Hz, 6H, Ar), 7.32–7.37 (m, 3H, PhSn), 7.70–7.80 (m, 2H, PhSn), 8.21 (d, J = 8.4 Hz, 6H, Ar). ¹³C-NMR (CDCl₃): δ 22.0 (CH₃), 127.5, 128.7, 128.9, 129.8, 131.1, 139.1, 145.4, 152.3, 238.2 (C=S). ¹¹⁹Sn-NMR (CDCl₃):

δ – 739.5. UV-vis (CH_2Cl_2) λ_{\max} (log ε): 221 (5.21), 258 (4.73), 340 (5.01), 445 (2.45) nm. Anal. Found: C, 51.72; H, 3.82. $\text{C}_{30}\text{H}_{26}\text{S}_6\text{Sn}$ Calc.: C, 51.65; H, 3.76%.

5e. Recrystallizing solvents: 1:1 CH_2Cl_2 –hexane; orange crystals (78%); m.p. 157–159°C. IR (KBr): 1269 (C=S), 1244 (C=S) cm^{-1} . $^1\text{H-NMR}$ (CDCl_3): δ 3.88 (s, 9H, CH_3O), 6.79 (d, J = 9.0 Hz, 6H, Ar), 7.34–7.41 (m, 3H, PhSn), 8.05–8.09 (m, 2H, PhSn), 8.32 (d, J = 9.0 Hz, 6H, Ar). $^{13}\text{C-NMR}$ (CDCl_3): δ 55.7 (CH_3O), 113.1, 128.8, 129.7, 130.1, 131.1, 134.9, 152.8, 165.1, 235.5 (C=S). $^{119}\text{Sn-NMR}$ (CDCl_3): δ – 748.2. UV-vis (CH_2Cl_2) λ_{\max} (log ε): 223 (5.13), 264 (4.69), 369 (4.95), 463 (2.47) nm. Anal. Found: C, 48.39; H, 3.56. $\text{C}_{30}\text{H}_{26}\text{O}_3\text{S}_6\text{Sn}$ Calc.: C, 48.32; H, 3.51%.

5f. Recrystallizing solvents: 2:4:7 CH_2Cl_2 – AcOEt –hexane; red crystals (53%); m.p. 137–140°C. IR (KBr): 1235 (C=S) cm^{-1} . $^1\text{H-NMR}$ (CDCl_3): δ 7.25–7.43 (m, 12H, Ar), 8.00–8.03 (m, 2H, PhSn), 8.21–8.23 (m, 3H, PhSn). $^{13}\text{C-NMR}$ (CDCl_3): δ 128.2, 128.7, 129.2, 130.2, 131.0, 139.8, 141.2, 151.5, 237.5 (C=S). $^{119}\text{Sn-NMR}$ (CDCl_3): δ – 739.8. UV-vis (CH_2Cl_2) λ_{\max} (log ε): 223 (5.14), 263 (4.72), 331 (4.65), 429 (2.45) nm. Anal. Found: C, 42.80; H, 2.31. $\text{C}_{27}\text{H}_{17}\text{Cl}_3\text{S}_6\text{Sn}$ Calc.: C, 42.73; H, 2.26%.

6a. Orange oil (86%). IR (neat): 1161 (C=S), 1132 (C=S) cm^{-1} . $^1\text{H-NMR}$ (CDCl_3): δ 2.92 (s, 3H, CH_3), 7.29–7.44 (m, 9H, PhPb), 7.57–7.68 (m, 6H, PhPb). $^{13}\text{C-NMR}$ (CDCl_3): δ 45.2 (CH_3), 128.3, 128.8, 135.9, 153.2 ($^1J_{\text{C-Pb}} = 541$ Hz), 259.9 (C=S). UV-vis (CH_2Cl_2) λ_{\max} (log ε): 222 (4.41), 270 (4.55), 334 (3.74), 470 (1.66) nm.

6b [2d]. Recrystallizing solvents: 5:4 CH_2Cl_2 –hexane; purple crystals (60%). $^1\text{H-NMR}$ (CDCl_3): δ 7.26 (t, J = 8.5 Hz, 1H, Ar), 7.33 (t, J = 7.6 Hz, 3H, PhPb), 7.45 (t, J = 7.6 Hz, 6H, PhPb), 7.50 (t, J = 8.5 Hz, 2H, Ar), 7.77 (d, J = 7.6 Hz, 6H, PhPb), 8.26 (d, J = 8.5 Hz, 2H, Ar). $^{13}\text{C-NMR}$ (CDCl_3): δ 127.5, 127.7, 128.5, 129.3, 130.1, 132.3, 137.0, 156.0 ($^1J_{\text{C-Pb}} = 544$ Hz), 235.4 (C=S). UV-vis (CH_2Cl_2) λ_{\max} (log ε): 222 (4.47), 271 (4.62), 303 (4.30), 519 (2.15) nm. Anal. Found: C, 50.89; H, 3.61. $\text{C}_{25}\text{H}_{20}\text{PbS}_2$ Calc.: C, 50.74; H, 3.41%.

6c [2d]. Recrystallizing solvents: 5:7 Et_2O –hexane; orange crystals (83%). $^1\text{H-NMR}$ (CDCl_3): δ 2.39 (s, 3H, CH_3), 7.08–7.15 (m, 4H, Ar), 7.34–7.53 (m, 9H, Ar), 7.64–7.92 (m, 6H, Ar). $^{13}\text{C-NMR}$ (CDCl_3): δ 19.8 (CH_3), 125.4, 125.7, 128.4, 129.4, 130.1, 130.6, 131.9, 137.0, 150.0, 155.6 ($^1J_{\text{C-Pb}} = 533$ Hz), 242.2 (C=S). UV-vis (CH_2Cl_2) λ_{\max} (log ε): 307 (3.83), 504 (2.23) nm. Anal. Found: C, 51.75; H, 3.90. $\text{C}_{26}\text{H}_{22}\text{PbS}_2$ Calc.: C, 51.55; H, 3.66%.

6d [2d]. Recrystallizing solvents: 3:2 CH_2Cl_2 –hexane; red crystals (88%). $^1\text{H-NMR}$ (CDCl_3): δ 2.34 (s, 3H, CH_3), 7.10 (d, J = 8.2 Hz, 2H, Ar), 7.36 (t, J = 7.6 Hz, 3H, PhPb), 7.48 (t, J = 7.6 Hz, 6H, PhPb), 7.78 (d, J = 7.6 Hz, 6H, PhPb), 8.20 (d, J = 8.2 Hz, 2H, Ar). $^{13}\text{C-NMR}$ (CDCl_3): δ 21.6 (CH_3), 127.8, 128.5, 129.3,

130.1, 137.0, 137.6, 143.4, 156.2 ($^1J_{\text{C-Pb}} = 543$ Hz), 234.5 (C=S). UV-vis (CH_2Cl_2) λ_{\max} (log ε): 222 (4.43), 272 (4.57), 318 (4.38), 520 (2.23) nm.

6e [2d]. Recrystallizing solvents: 5:3 CH_2Cl_2 –hexane; red crystals (78%). $^1\text{H-NMR}$ (CDCl_3): δ 3.68 (s, 3H, CH_3O), 6.86 (d, J = 9.0 Hz, 2H, Ar), 7.29 (t, J = 7.3 Hz, 3H, PhPb), 7.42 (t, J = 7.3 Hz, 6H, PhPb), 7.78 (d, J = 7.3 Hz, 6H, PhPb), 8.34 (d, J = 9.0 Hz, 2H, Ar). $^{13}\text{C-NMR}$ (CDCl_3): δ 55.3 (CH_3O), 112.7, 127.4, 129.3, 129.9, 136.8, 138.4, 156.2 ($^1J_{\text{C-Pb}} = 545$ Hz), 163.6, 232.0 (C=S). UV-vis (CH_2Cl_2) λ_{\max} (log ε): 222 (4.44), 272 (4.62), 344 (4.45), 515 (2.32) nm. Anal. Found: C, 50.39; H, 3.62. $\text{C}_{26}\text{H}_{22}\text{OPbS}_2$ Calc.: C, 50.22; H, 3.57%.

6f [2d]. Recrystallizing solvents: 2:1 CH_2Cl_2 –hexane; red crystals (73%). $^1\text{H-NMR}$ (CDCl_3): δ 7.18 (d, J = 8.5 Hz, 2H, Ar), 7.31 (t, J = 7.6 Hz, 3H, PhPb), 7.44 (t, J = 7.6 Hz, 6H, PhPb), 7.76 (d, J = 7.6 Hz, 6H, PhPb), 8.17 (d, J = 8.5 Hz, 2H, Ar). $^{13}\text{C-NMR}$ (CDCl_3): δ 127.8, 128.8, 129.4, 130.1, 136.9, 138.0, 143.7, 155.9 ($^1J_{\text{C-Pb}} = 544$ Hz), 233.2 (C=S). UV-vis (CH_2Cl_2) λ_{\max} (log ε): 221 (4.43), 272 (4.71), 313 (4.34), 524 (2.18) nm. Anal. Found: C, 47.99; H, 3.11. $\text{C}_{25}\text{H}_{19}\text{ClPbS}_2$ Calc.: C, 47.95; H, 3.06%.

7a. Recrystallizing solvents: hexane; orange crystals (35%); m.p. 87–88°C. IR (KBr): 1162 (C=S), 1152 (C=S) cm^{-1} . $^1\text{H-NMR}$ (CDCl_3): δ 2.67 (s, 6H, CH_3), 7.31 (t, J = 7.5 Hz, 2H, PhPb), 7.44 (t, J = 7.5 Hz, 4H, PhPb), 7.92 (d, J = 7.5 Hz, 4H, PhPb). $^{13}\text{C-NMR}$ (CDCl_3): δ 44.9 (CH_3), 129.5, 130.2, 136.7, 137.0, 250.7 (C=S). UV-vis (CH_2Cl_2) λ_{\max} (log ε): 222 (4.61), 270 (4.54), 335 (4.41), 467 (2.11) nm.

7b. Recrystallizing solvents: 2:1 CH_2Cl_2 –hexane; orange crystals (74%); m.p. 196–198°C. IR (KBr): 1217 (C=S) cm^{-1} . $^1\text{H-NMR}$ (CDCl_3): δ 7.38 (t, J = 7.7 Hz, 4H, PhPb), 7.42 (t, J = 7.8 Hz, 4H, Ar), 7.51 (t, J = 7.7 Hz, 2H, PhPb), 7.56 (t, J = 7.8 Hz, 2H, Ar), 7.95 (d, J = 7.7 Hz, 4H, PhPb), 8.09 (d, J = 7.8 Hz, 4H, Ar). $^{13}\text{C-NMR}$ (CDCl_3): δ 128.3, 129.0, 130.2, 130.5, 133.5, 135.1, 138.4, 157.8, 243.3 (C=S). UV-vis (CH_2Cl_2) λ_{\max} (log ε): 222 (4.49), 272 (4.09), 316 (4.49), 472 (2.67) nm. Anal. Found: C, 46.82; H, 3.11. $\text{C}_{26}\text{H}_{20}\text{PbS}_4$ Calc.: C, 46.76; H, 3.02%.

7c. Recrystallizing solvents: 4:5 Et_2O –hexane; orange crystals (83%); m.p. 211–214°C. IR (KBr): 1230 (C=S) cm^{-1} . $^1\text{H-NMR}$ (CDCl_3): δ 2.35 (s, 6H, CH_3), 7.10 (t, J = 7.3 Hz, 4H, Ar), 7.20 (t, J = 7.3 Hz, 2H, Ar), 7.33 (d, J = 7.3 Hz, 2H, Ar), 7.44 (t, J = 7.5 Hz, 2H, PhPb), 7.57 (t, J = 7.5 Hz, 4H, PhPb), 8.16 (d, J = 7.5 Hz, 4H, PhPb). $^{13}\text{C-NMR}$ (CDCl_3): δ 20.0 (CH_3), 125.5, 125.8, 129.0, 130.0, 130.3, 130.8, 132.1, 134.4, 151.1, 161.1, 244.0 (C=S) nm. Anal. Found: C, 48.42; H, 3.57. $\text{C}_{28}\text{H}_{24}\text{PbS}_4$ Calc.: C, 48.32; H, 3.48%.

7d. Recrystallizing solvents: 2:1 CH_2Cl_2 –hexane; orange crystals (83%); m.p. 214–217°C. IR (KBr): 1222 (C=S) cm^{-1} . $^1\text{H-NMR}$ (CDCl_3): δ 2.35 (s, 6H, CH_3), 7.13 (d, J = 8.2 Hz, 4H, Ar), 7.35 (t, J = 7.3 Hz, 2H,

PhPb), 7.49 (t, $J = 7.3$ Hz, 4H, PhPb), 8.11 (d, $J = 7.3$ Hz, 4H, PhPb), 8.20 (d, $J = 8.2$ Hz, 4H, Ar). ^{13}C -NMR (CDCl_3): δ 21.7 (CH_3), 127.2, 128.4, 129.2, 129.4, 130.0, 130.7, 134.9, 144.4, 239.4 (C=S). UV-vis (CH_2Cl_2) λ_{\max} (log ϵ): 222 (4.44), 273 (4.06), 333 (4.70), 474 (2.70) nm. Anal. Found: C, 48.37; H, 3.52. $\text{C}_{28}\text{H}_{24}\text{PbS}_4$ Calc.: C, 48.32; H, 3.48%.

7e. Recrystallizing solvents: 3:2 CH_2Cl_2 –hexane; orange crystals (82%); m.p. 209–211°C. IR (KBr): 1261 (C=S), 1235 (C=S) cm^{-1} . ^1H -NMR (CDCl_3): δ 3.89 (s, 6H, CH_3O), 6.91 (d, $J = 9.0$ Hz, 2H, Ar), 7.44 (t, $J = 7.8$ Hz, 4H, PhPb), 7.50 (t, $J = 7.8$ Hz, 2H, PhPb), 8.01 (d, $J = 7.8$ Hz, 4H, PhPb), 8.19 (d, $J = 9.0$ Hz, 2H, Ar). ^{13}C -NMR (CDCl_3): δ 55.6 (CH_3O), 113.6, 129.2, 129.5, 129.6, 129.8, 135.7, 137.6, 164.0, 243.1 (C=S). UV-vis (CH_2Cl_2) λ_{\max} (log ϵ): 222 (4.43), 271 (4.11), 348 (4.71), 470 (2.73) nm. Anal. Found: C, 46.27; H, 3.37. $\text{C}_{28}\text{H}_{24}\text{O}_2\text{PbS}_4$ Calc.: C, 46.20; H, 3.32%.

7f. Recrystallizing solvents: 4:3 CH_2Cl_2 –hexane; orange crystals (85%); m.p. 194–197°C. IR (KBr): 1226 (C=S) cm^{-1} . ^1H -NMR (CDCl_3): δ 7.38 (d, $J = 7.7$ Hz, 4H, Ar), 7.42–7.52 (m, 6H, PhPb), 7.91–7.98 (m, 4H, PhPb), 8.01 (d, $J = 7.7$ Hz, 4H, Ar). ^{13}C -NMR (CDCl_3): δ 128.5, 128.8, 128.9, 129.0, 129.3, 130.2, 135.0, 140.1, 247.9 (C=S). UV-vis (CH_2Cl_2) λ_{\max} (log ϵ): 222 (4.47), 272 (4.21), 322 (4.72), 478 (2.76) nm. Anal. Found: C, 42.40; H, 2.51. $\text{C}_{26}\text{H}_{18}\text{Cl}_2\text{PbS}_4$ Calc.: C, 42.38; H, 2.46%.

4.2. General procedure for reaction of SnCl_4 with piperidinium or sodium 4-methylbenzenecarbodithioate

To a solution of piperidinium 4-methylbenzenecarbodithioate (1.016 g, 4.00 mmol) in CH_2Cl_2 (30 ml), $\text{SnCl}_4\text{-CH}_2\text{Cl}_2$ 1.0 M solution (1.0 ml, 1.0 mmol) was added and the mixture was stirred at 20°C for 1 h. The solvent was removed under reduced pressure (20°C/2.7 kPa). The mixtures were dissolved into a solvent of CH_2Cl_2 (15 ml). Filtration of the resulting precipitate gave a mixture of dichlorotin bis(4-methylbenzenecarbodithioate) and bis(4-methylthiobenzoyl) disulfide [3] as orange solid. Fractional crystallization of the solid gave chemically pure dichlorotin bis(4-methylbenzenecarbodithioate) in 8% yield: Yellow crystals; m.p. 191–193°C. IR (KBr): 1249 (C=S), 1228 (C=S) cm^{-1} . ^1H -NMR (CDCl_3): δ 2.46 (s, 6H, CH_3), 7.25 (d, $J = 8.3$ Hz, 4H, Ar), 8.14 (d, $J = 8.3$ Hz, 4H, Ar). ^{13}C -NMR (CDCl_3): δ 22.2 (CH_3), 128.1, 129.4, 135.9, 149.1, 237.0 (C=S). ^{119}Sn -NMR (CDCl_3): δ –715.3. Anal. Found: C, 36.40; H, 2.61. $\text{C}_{16}\text{H}_{14}\text{Cl}_2\text{S}_4\text{Sn}$ Calc.: C, 36.66; H, 2.69%.

4.3. Preparation of single crystals

1d (0.124 g) was crystallized from CH_2Cl_2 (0.4 ml),

Et_2O (0.1 ml), and hexane (0.5 ml) at 25°C for 6 days. **3d** (0.151 g) was crystallized from CH_2Cl_2 (0.6 ml), Et_2O (0.1 ml), and hexane (0.5 ml) at 25°C for 5 days. **4d** (0.120 g) was crystallized from CH_2Cl_2 (0.5 ml), Et_2O (0.3 ml), and hexane (0.5 ml) at 25°C for 10 days. **5c** (0.107 g) was crystallized from CH_2Cl_2 (0.6 ml) and hexane (0.5 ml) at 25°C for 9 days. **6d** (0.131 g) was crystallized from CH_2Cl_2 (0.8 ml), Et_2O (0.3 ml), and hexane (0.5 ml) at 25°C for 2 weeks.

4.4. X-ray structural analysis

The measurements were carried out on a Rigaku AFC7R four-circle diffractometer with graphite-monochromated Mo– K_α ($\lambda = 0.71069$ Å) and Cu– K_α radiation ($\lambda = 1.54178$ Å). All of the structures were solved and refined using the TEXSAN® crystallographic software package on an IRIS Indigo computer. Lorentz and polarization corrections were applied to the data, and empirical absorption corrections (DIFABS [19] (**3d**, **4d**, **5c**, and **6d**) and Ψ -scans [20] (**1d**)) were also applied. The structures were solved by direct method using SHELXS-86 [21] for **1d**, **3d**, **4d**, **5c**, and **6d** and expanded using DIRIDIF-94 [22]. Scattering factors for neutral atoms were from Cromer and Waber [23] and anomalous dispersion [24] was used. Crystal data and measurement description are summarized in Table 2.

5. Supplementary material

Crystallographic data for the structural analysis have been deposited at the Cambridge Crystallographic Data Centre (no. CCDC 139447 for compound **1d**, CCDC 139448 for compound **3d**, CCDC 139449 for compound **4d**, CCDC 139450 for compound **5c** and CCDC 139451 for compound **6d**). Copies of this information maybe obtained free of charge from The Director, CCDC, 12 Union Road, Cambridge CB2 1EZ, UK (Fax: +44-1223-336033; e-mail: or www: <http://www.ccdc.cam.ac.uk>).

Acknowledgements

This research was supported by a Grant-in-Aid for Scientific Research on Priority Areas (No. 09239220) and by a Grants-in-Aid for Scientific Research (No. 09355032) from the Ministry of Education, Science, Sports and Culture of Japan. We thank Professor Takashi Kawamura and Associate Professor Masahiro Ebihara of Gifu University for their invaluable assistance with X-ray crystallography.

References

- [1] (a) G.D. Thorn, R.A. Ludwig, *The Dithiocarbamates and Related Compounds*, Elsevier, Amsterdam, 1962. (b) D. Coucovanis, *Prog. Inorg. Chem.* 11 (1970) 233. (c) D. Coucovanis, *Prog. Inorg. Chem.* 26 (1979) 301. (d) I. Haiduc, *Rev. Inorg. Chem.* 3 (1981) 353.
- [2] (a) S. Kato, M. Mizuta, Y. Ishii, *J. Organomet. Chem.* 55 (1973) 121. (b) S. Kato, T. Kato, Y. Shibashashi, E. Kakudo, M. Mizuta, Y. Ishii, *J. Organomet. Chem.* 76 (1974) 215. (c) S. Kato, A. Hori, H. Shiotani, M. Mizuta, N. Hayashi, T. Takakuwa, *J. Organomet. Chem.* 82 (1974) 223. (d) T. Katada, S. Kato, M. Mizuta, *Chem. Lett.* (1975) 1037. (e) S. Kato, A. Hori, M. Mizuta, T. Katada, H. Ishihara, *J. Organomet. Chem.* 420 (1991) 13. (f) S. Kato, N. Kitaoka, O. Niyomura, Y. Kitoh, T. Kanda, M. Ebihara, *Inorg. Chem.* 38 (1999) 496.
- [3] (a) S. Kato, T. Kato, T. Kataoka, M. Mizuta, *Int. J. Sulfur Chem.* 8 (1973) 437. (b) O. Niyomura, Y. Kitoh, K.-I. Nagayama, S. Kato, *Sulfur Lett.* 22 (1999) 195.
- [4] Covalent bond radii: C–S 1.81 Å, C=S 1.61, Ge–S 2.26, Sn–S 2.44, Pb–S 2.58 Å. L. Pauling, *The Chemical Bond*, Cornell University Press, Ithaca, New York, 1976.
- [5] J.E. Drake, A.G. Mislankar, M.L.Y. Wong, *Inorg. Chem.* 30 (1991) 2174.
- [6] (a) V.G.D. Kumar, C. Wei, E. Sinn, *J. Organomet. Chem.* 290 (1985) 291. (b) D. Dakternieks, H. Zhu, D. Masi, C. Mealli, *Inorg. Chem.* 31 (1992) 3601.
- [7] E.R.T. Tiekkink, *J. Organomet. Chem.* 314 (1986) 85.
- [8] F.A.K. Nasser, A. Wilson, Jr., J.J. Zuckermann, *Organometallics* 4 (1985) 2073.
- [9] M.G. Begley, P.G.C. Gaffney, A.S. Harrisona, *J. Organomet. Chem.* 289 (1985) 281.
- [10] S.N. Olafsson, T.N. Petersen, P. Andersen, *Acta Chem. Scand.* 50 (1996) 745.
- [11] Sum of van der Waals radii: Ge···S 3.78 Å, Sn···S 3.96 Å, Pb···S 3.82 Å. A. Bondi, *J. Phys. Chem.* 68 (1964) 441.
- [12] (a) T. Kimura, N. Yasuoka, N. Kasai, M. Kakudo, *Bull. Chem. Soc. Jpn.* 45 (1972) 1649. (b) T.P. Lockhart, W.F. Manders, E.O. Schlemper, J.J. Zuckermann, *J. Am. Chem. Soc.* 108 (1986) 4074.
- [13] P. Singh, S. Bhattacharya, V.D. Gupta, H. Nöth, *Chem. Ber.* 129 (1996) 1093.
- [14] J. Potenza, D. Mastropalo, *Acta Crystallogr. Sect. B* 29 (1973) 1830.
- [15] P.F.R. Ewings, P.G. Harrison, T.J. King, *J. Chem. Soc. Dalton Trans.* (1976) 1399.
- [16] (a) J.S. Morris, E.O. Schlemper, *J. Cryst. Mol. Struct.* 8 (1978) 295. (b) J.S. Morris, E.O. Schlemper, *J. Cryst. Mol. Struct.* 9 (1979) 1. (c) D. Dakternieks, H. Zhu, D. Masi, C. Mealli, *Inorg. Chim. Acta* 211 (1993) 155. (d) E. Kello, V. Vrabel, I. Skacan, J. Holecek, *Acta Crystallogr. Sect. C* 51 (1995) 408.
- [17] M.J. Barrow, E.A.V. Ebsworth, C.M. Huntley, D.W.H. Rankin, *J. Chem. Soc. Dalton Trans.* (1982) 1131.
- [18] S. Kato, T. Mitani, M. Mizuta, *Int. J. Sulfur Chem.* 8 (1973) 359.
- [19] N. Walker, D. Stuart, *Acta Crystallogr. Sect. A* 39 (1983) 158.
- [20] G.M. Sheldrick, in: G.M. Sheldrick, C. Kruger, R. Goddard (Eds.), *Crystallographic Computing 3*, vol. 3, Oxford University Press, UK, 1985, p. 175.
- [21] A.C.T. North, D.C. Phililips, F.S. Mathews, *Acta Crystallogr. Sect. A* 24 (1986) 351.
- [22] The DIRIDIF-94 program system was used; P.T. Beukens, G. Admiraal, G. Beurskiens, W.P. Bosman, R. de Gelder, R. Israel, J.M.M. Smits, Technical Report of the Crystallography Laboratory, University of Nijmegen, The Netherlands, 1994.
- [23] D.T. Cromer, J.T. Waber, *International Tables for X-ray Crystallography*, vol. IV, Kynoch, Birmingham, UK, 1974, Table 2.2A.
- [24] D.C. Creagh, W.J. McAuley, in: A.J.C. Wilson (Ed.), *International Tables for X-ray Crystallography*, vol. C, Kluwer, Boston, 1992, Table 4.2.6.8, pp. 219.